ACS chemical biology

Letters

pubs.acs.org/acschemicalbiology

Template-Assisted and Self-Activating Clicked Peptide as a Synthetic Mimic of the SH2 Domain

Katsunori Tanaka,*[,†] Sanae Shirotsuki,[†] Takayuki Iwata,[†] Chika Kageyama,[†] Tsuyoshi Tahara,[‡] Satoshi Nozaki,[‡] Eric R. O. Siwu,[†] Satoru Tamura,[§] Shunsuke Douke,[§] Nobutoshi Murakami,[§] Hirotaka Onoe,[‡] Yasuyoshi Watanabe,[‡] and Koichi Fukase*[,†]

[†]Department of Chemistry, Graduate School of Science, Osaka University, 1-1 Machikaneyama-cho, Toyonaka-shi, Osaka 560-0043, Japan

[‡]RIKEN Center for Molecular Imaging Science, 6-7-3 Minatojima-minamimachi, Chuo-ku, Kobe-shi, Hyogo 650-0047, Japan

[§]Graduate School of Pharmaceutical Sciences, Osaka University, 1-6 Yamada-oka, Suita-shi, Osaka 565-0871, Japan

Supporting Information

ABSTRACT: A new synthetic strategy for obtaining artificial receptors that selectively regulate and/or control specific protein/protein interactions was developed based on the template-assisted and the self-activating click reaction applied to a combinatorial library. Synthetic mimics of the Grb2-SH2 domain, examined as a model case, selectively bound to a target signaling protein to induce cytotoxicity and inhibit tumor growth *in vivo*.

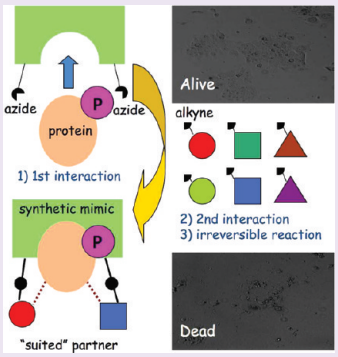

Exploring efficient strategies for identifying the molecules that selectively regulate protein/protein interactions is one of the most actively studied topics in chemical biology.[1−16] The selective activation and/or inhibition of specific phosphorylation-mediated protein/protein interactions within a signaling pathway[17−21] may direct a specific biological response on the cellular level. Such molecules can selectively control cell fate, *e.g.*, of a target cancer cell in which a characteristic protein phosphorylation event dominantly regulates the growth, proliferation, and death of the cell.

Growth factor receptor-bound protein 2 (Grb2)[22−24] is an adaptor protein that plays a critical role in downstream MAPK signaling. Grb2 signaling is initiated by phosphorylation of the receptor tyrosine kinases. The Src homology (SH2) domain of Grb2 preferentially binds to the phosphotyrosine with the sequence motif *p*YVNV, while the two SH3 domains flanking the SH2 domain bind to the Ras exchange factor Sos. Both interactions catalyze GTP/GDP exchange, thereby activating the GTPase and the downstream MAPK cascade.[22−24] Because receptor tyrosine kinases are overexpressed in some cancer cells, the subsequent downstream MAPK cascades dominantly regulate cell proliferation. Disruption of the phosphotyrosine/Grb2-SH2 interaction is, therefore, an attractive target for drug discovery in the field of oncology.[25−28] A large number of antagonists against the SH2 domain have been designed based on the SH2-recognizing motif (*p*YVNV) in conjunction with linear or cyclic peptide scaffolds.[29−35] The opposite approach to inhibiting the interaction would involve using SH2 domain mimics, and this approach has not been extensively tested. Despite the availability of X-ray crystallographic data that characterizes the interaction,[30,36−39] the design of such protein mimics is far more difficult than the conformation-fixing approach represented by the SH2-recognizing motif with a known peptide sequence, *p*YVNV. Besides the continuous trials on developing the selective SH2 domain ligands,[28] the opposite approach may provide a new strategy for inhibiting a particular signaling pathway, namely, *via* selective interactions between the SH2 domain mimic and a particular phosphoprotein among many phosphoproteins that can interact with the target SH2 domain; the method could offer more general and flexible solutions to designing the artificial receptors, namely, the tailor-made synthesis of small molecules that selectively inhibit, control, and regulate the desired protein/protein interactions.

In this Letter, we describe an approach for obtaining artificial receptors using the Grb2-SH2 domain mimic as a case study. The synthetic peptide was efficiently produced by the template-assisted and self-activating Huisgen 1,3-dipolar cycloaddition using a dynamic combinatorial library. The clicked product thus obtained internalized into the cancer cells A431, selectively bound to the Grb2-SH2 interacting proteins, and selectively induced cytotoxicity in the cancer cell both *in vitro* and *in vivo*.

Received: November 23, 2010
Accepted: January 12, 2012
Published: January 12, 2012

   dx.doi.org/10.1021/cb2003175 | *ACS Chem. Biol.* 2012, 7, 637−645

The template-assisted strategy, illustrated in Figure 1, is based on our earlier finding that the bis-lysine-based peptide **1** interacts with a phosphate group (see also the structures presented in Scheme 1).[40] As the bis-lysine **1** coordinates to a template phosphorylated protein (Figure 1, step a), the template is made to additively interact with a certain peptide library **2** during the dynamic processing step (step b) (see ref 41, a representative example of dynamic combinatorial chemistry applied to development of enzyme inhibitors; see also refs 50−59). Bis-lysine **1** is then irreversibly modified by the peptide partners that are most suited to the template protein (step c) such that the resulting products show higher affinity and selectivity toward the template protein than the bis-lysine **1**.

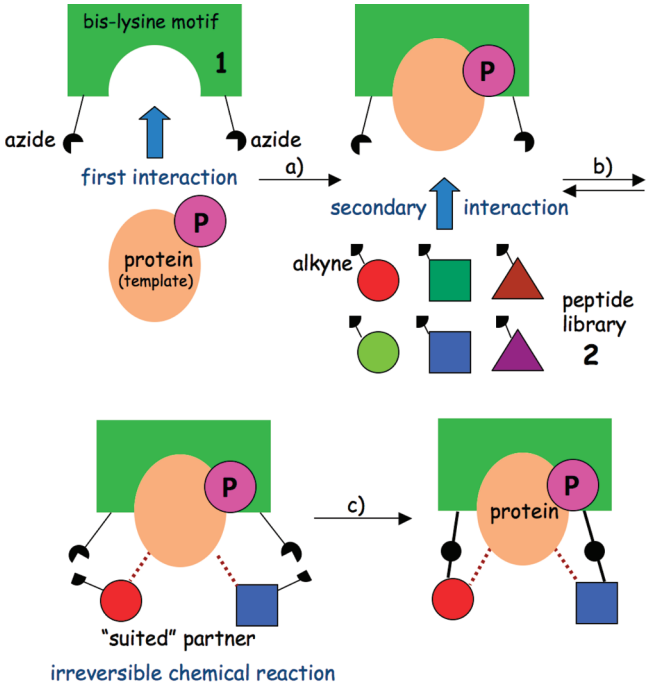

Figure 1. Concept of template-assisted synthesis of the SH2 domain mimic.

To efficiently produce the template-assisted products, namely, the products being templated by the *p*YVNV motif of a phosphorylated protein, the cyclic peptide **3a**[30] (Scheme 1) was used as a template in place of the entire protein. Peptide **3a** has been reported to strongly and selectively bind to the Grb2-SH2 domain (IC_{50} = 0.52 ± 0.20 μM).[30] The amino acids composing the peptide library **2** were selected on the basis of the X-ray crystallographic structure between the Grb2-SH2 domain and the peptide **3a** or similar analogues.[30,36−39] Phe, Leu, and Trp were included to account for the hydrophobic interactions, whereas His, Ser, and Asn were introduced for the hydrogen-bonded interactions. Irreversible modification of **1** by the peptide library **2** was accomplished using the Cu(I)-mediated Huisgen 1,3-dipolar cycloaddition (Sharpless/Meldal click reaction).[42−49] Although the Cu(I)-catalyzed azide/acetylene ligation has successfully been applied to the dynamic combinatorial synthesis of small molecule-based enzyme

Scheme 1. Template-Assisted Synthesis of a Grb2-SH2 Domain Mimic[a]

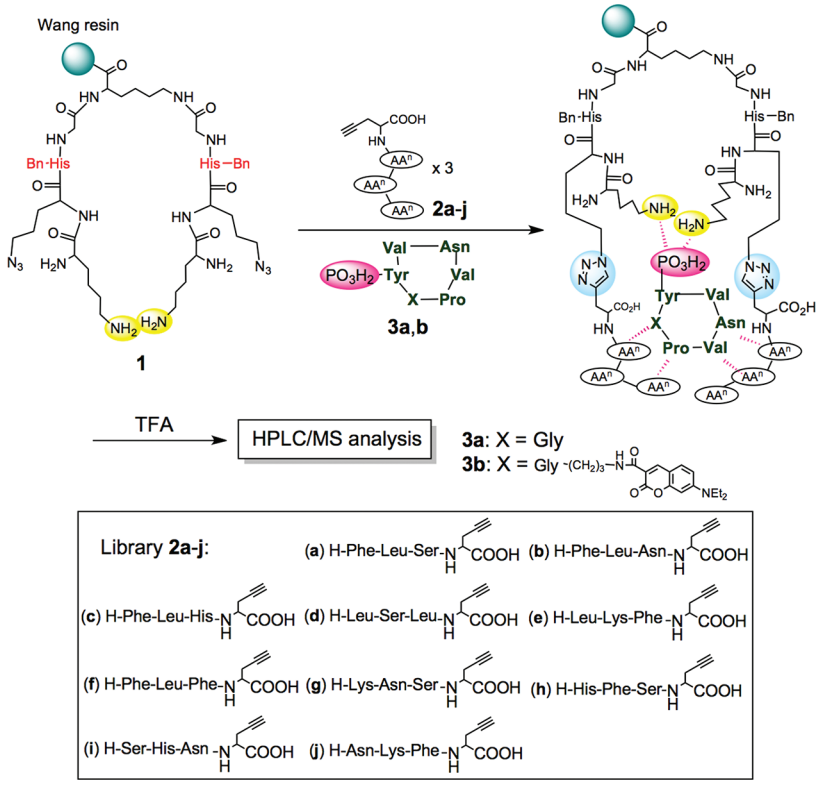

[a]Bis-lysine **1** on resin (1.0 μmol) was reacted with three acetylene peptides **2a−j** (each 2 equiv) and CuI (6 equiv) in a mixed solvent system of H_2O, MeCN, DMF, and THF (5:5:8:72) at rt for 5 d. The reaction was performed in the presence or absence of peptide **3a** (1 equiv). After cleavage from the resin by TFA treatment, the composition of the clicked product mixture was analyzed by HPLC and ESI-MS.

dx.doi.org/10.1021/cb2003175 | *ACS Chem. Biol.* 2012, 7, 637−645

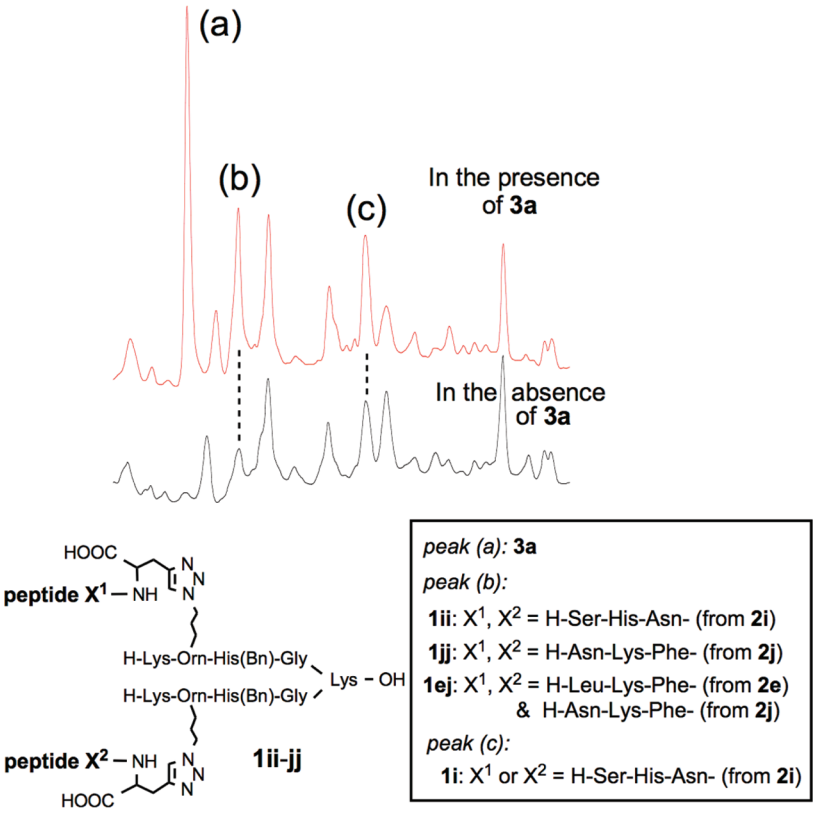

Figure 2. HPLC analysis of clicked products (column; Nacalai tesque $5C_{18}$-AR300, 4.6 × 250 mm, MeCN in H_2O (0.05% TFA), detection at 210 nm). (a) Phosphorylated peptide **3a**. (b) Bis-clicked products **1ii**, **1jj**, or **1ej** as possible candidates. (c) Monoclicked products **1i**.

inhibitors,[50−59] the peptide-based reaction remains challenging due to coordination of the copper ions to the peptide backbone,[48] which inhibits the reaction. We therefore purposely introduced a benzyl histidine[60] adjacent to the azide moiety in **1** (Scheme 1). This moiety efficiently coordinated the copper ions and brought the reactive sites (azide and acetylene) into proximity to enhance the ligation efficiency.[61]

A template-assisted and self-activating click reaction was then performed on a solid support under conditions established previously in this laboratory.[60] The solid-support protocol was selected because the clicked products, which strongly interacted with the cyclic peptide **3a**, could be easily and rapidly identified after cleavage of the products from the resin (*vide infra*, Scheme 1). Thus, the bis-lysine **1** on the Wang resin (1.0 μmol) was treated with CuI (6 equiv) and the three acetylenes (each 2 equiv), which were randomly selected from the library **2a**−**j** in the presence of peptide **3a** (1 equiv) in a mixed solvent containing H_2O, MeCN, DMF, and THF (5:5:8:72). It should be noted that the click conditions employed here, especially when both CuI as the copper source[47] and acetonitrile as the solvents[49] were used, slow the cycloaddition reaction, hence giving rise to the sluggish reactions (see Figure 2 and Supplementary Figure S2, *vide infra*). By keeping the click reaction slow, we could minimize the background reaction and therefore efficiently detect the "templated" products.

After the mixture was shaken for 5 days, the excess reagents were washed away, the remaining copper ions were removed by chelating to DOTA (1,4,7,10-tetraazacyclodecane-1,4,7,10-tetraacetic acid),[61−63] and the clicked peptides were cleaved from the resin by acid treatment. The composition of the resulting product mixture was analyzed by HPLC and ESI-MS and was compared with those mixtures produced in the absence of **3a** (Figure 2). By performing the click reaction using 18 combinations of the three peptides from library **2**, we could screen a theoretical number of 120 clicked products, *i.e.*, the bis-clicked products (homo- and hetero-products) and mono-clicked products with the positional isomers. We do not need to prepare all possible compounds, but the desired "templated products" could selectively be produced by the system.

Of the 18 template-assisted reactions, one case displayed distinctly different HPLC profiles in the presence or absence of the peptide **3a**. The template-assisted reaction that included the combined peptides **2e**, **2i**, and **2j** yielded increased peak intensities (at positions b and c in Figure 2) in the presence of **3a**. ESI-MS analysis of peak (b) detected the molecular ions of 539.3, 570.2, 718.8, 752.3, and 759.6, thereby suggesting the presence of either the homo-bis-clicked product with two molecules of **2i** (**1ii**; $[M + 4H]^{4+}$ = 539.3 and $[M + 3H]^{3+}$ = 718.7), the homo-bis-clicked product with **2j** (**1jj**; $[M + Na + 3H]^{4+}$ = 570.3, $[M + 3H]^{3+}$ = 752.7, and $[M + Na + 2H]^{3+}$ = 760.1), or the mixed-bis-clicked product with **2e** and **2j** (**1ej**; $[M + Na + 3H]^{4+}$ = 570.1, $[M + 3H]^{3+}$ = 752.4, and $[M + Na + 2H]^{3+}$ = 759.7). The exact structures corresponding to the peak b could not be elucidated at this stage because the MS analysis was complicated by their similar molecular weights, the various ion adducts, and the highly charged ESI ionization. In contrast, the signal c corresponding to the molecular ions at 851.4 was identified as the mono-clicked product with **2i** (**1i**; $[M + 2H]^{2+}$ = 851.9). It should be noted that the peak a, corresponding to the peptide **3a** was detected in the HPLC spectrum, *i.e.*, the clicked products produced by this approach were expected to strongly bind to **3a** such that **3a** could not be washed from the

dx.doi.org/10.1021/cb2003175 | *ACS Chem. Biol.* 2012, 7, 637−645

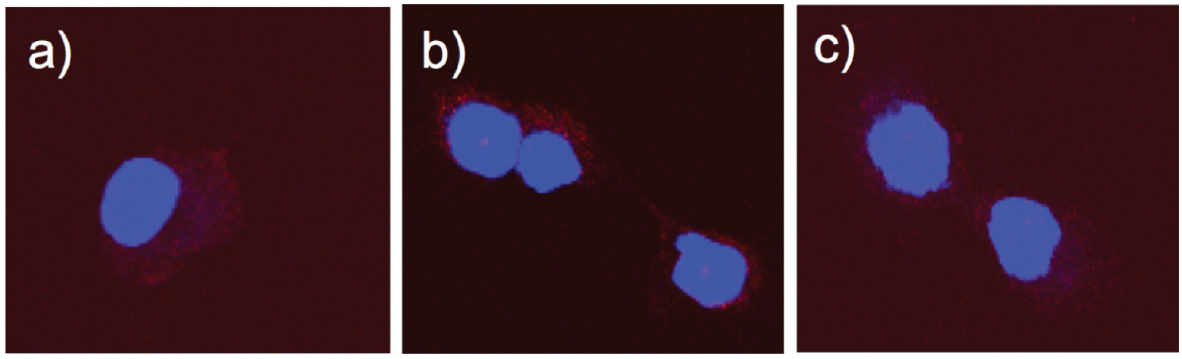

Figure 3. Confocal microscopy images of A431 cells treated with the TAMRA-labeled **1ii** and **1** for 16 h at 37 °C (DAPI detection for nuclei). (a) 1.4 μM TAMRA-labeled **1ii**. (b) 2.1 μM TAMRA-labeled **1ii**. (c) 3.2 μM TAMRA-labeled **1**. Average fluorescence intensity per each cell is (a) 231, (b) 448, and (c) 248. Low fluorescence/background ratio in images (a) and (c) is due to the weak fluorescence. TAMRA: carboxytetramethylrhodamine.

resin, even by repeated washing procedures on the solid supports.

To confirm that the clicked products **1ii**, **1jj**, **1ej**, or **1i** were the **3a**-assisted products, bis-lysine **1** immobilized on the Wang resin was treated with a single peptide **2i** in the presence or absence of **3a** (Supplementary Figure S2). Although the clicked product **1ii** could not be observed in the absence of this template, it was produced in the presence of **3a**. The results clearly showed that the template **3a** assisted the production of **1ii**, **1jj**, **1ej**, or **1i** (Figure 2), strongly suggesting that these products provided an optimal fit to the peptide **3a** and that they may possibly act as Grb2-SH2 mimics. Because (1) bis-derivatives **1ii** and **1jj** were the major products by the templated approach (Figure 2 and Supplementary Figure S2), and (2) the mono-clicked product **1i** (as positional isomers) and the mixed-bis-clicked product **1ej** could not readily be prepared by straightforward methods, we focused only on the K_d and the biological properties of the homo-bis-clicked products.

The dissociation constants (K_d) of the **3a**-assisted clicked products were determined using the 7-dialkylaminocoumarin-labeled fluorescence peptide **3b** (structure shown in Scheme 1); we knew that the position of the coumarin fluorophore in **3b** does not inhibit the interaction according to the earlier report.[30] Our fluorescence-based analysis below also experimentally showed the interaction with the templated products, but not with the parent analogue **1** (*vide infra*). Titrations of **3b** with the clicked products **1ii**, **1jj**, and the simple bis-lysine peptide **1** were followed by monitoring the fluorescence spectrum of **3b** (see ref 64, 7-alkylaminocoumar as a detection tag for biomolecule interaction). Although significant changes in the coumarin fluorescence (excitation at 420 nm, emission at 460 nm) were observed upon addition of the clicked products **1ii** and **1jj**, no spectral changes were detected in the presence of peptide **1** (Supplementary Figure S3). This result confirmed that **3a** specifically interacted with the **3a**-assisted products.[64] Scatchard plots were prepared according to the titration spectra (Supplementary Figure S4),[65−67] and the values of K_d were calculated to be 1.5 ± 0.90 μM (**1ii**) and 2.4 ± 0.51 μM (**1jj**).

With the template-assisted products with micromolar-level K_d values in hand, we next examined their biological properties using the A431 cancer cell line, in which EGFR (epidermal growth factor receptor), one of the tyrosine kinase receptor families, is overexpressed and critically regulates cell proliferation.[68] Fluorescently labeled and biotin-labeled probes of **1ii** (Supplementary Figures S5 and S8) were used to investigate (i) internalization within the cell, (ii) selectivity to the signaling proteins, and (iii) the biological effects on the A431 cells.

As shown in Figure 3, TAMRA-labeled **1ii** was internalized into the A431 cell in a dose-dependent manner and was distributed to the cytoplasm by incubation at 37 °C for 16 h (Figure 3a,b; also see Supplementary Figure S5). Interestingly, TAMRA-labeled **1**, which was a precursor for the template-assisted click reaction, was less effective at internalization (Figure 3c). Addition of histidine moiety to the bis-lysine peptide **1** might increase the efficiency of internalization of **1ii**, presumably due to an increase in the peptide basicity.[69−71]

Proteins that may have interacted with peptide **1ii** in the A431 lysate were then fished out using the biotin-probe (Figure 4). SDS-PAGE/reverse staining[72,73] of the avidin bead extracts[74−76] detected a low intensity but more distinct band at 65 kDa than that in the control extracts (Figure 4A, lanes (b) and (c)). The biotin/avidin extracts were further analyzed using the six antibodies against the proteins involved in phosphorylation in the EGFR-mediated signaling pathway (see the Supporting Information for a detailed procedures and

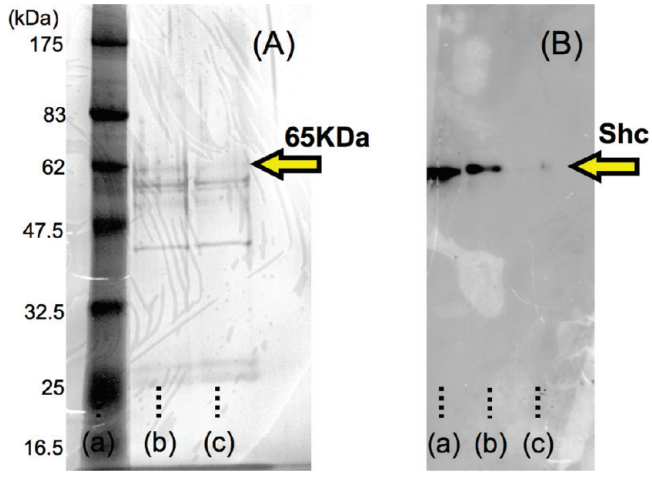

Figure 4. SDS-PAGE of the A431 lysate after treatment with the biotin-probe **1ii**. (A) Reverse staining: (a) marker; (b) treatment with 100 μM biotin-labeled **1ii**; (c) control (treatment with H_2O instead of the biotin probe). (B) Western blot and anti-Shc antibody detection: (a) treatment with 300 μM biotin-labeled **1ii**; (b) treatment with 100 μM biotin-labeled **1ii**; (c) control.

dx.doi.org/10.1021/cb2003175 | *ACS Chem. Biol.* 2012, 7, 637−645

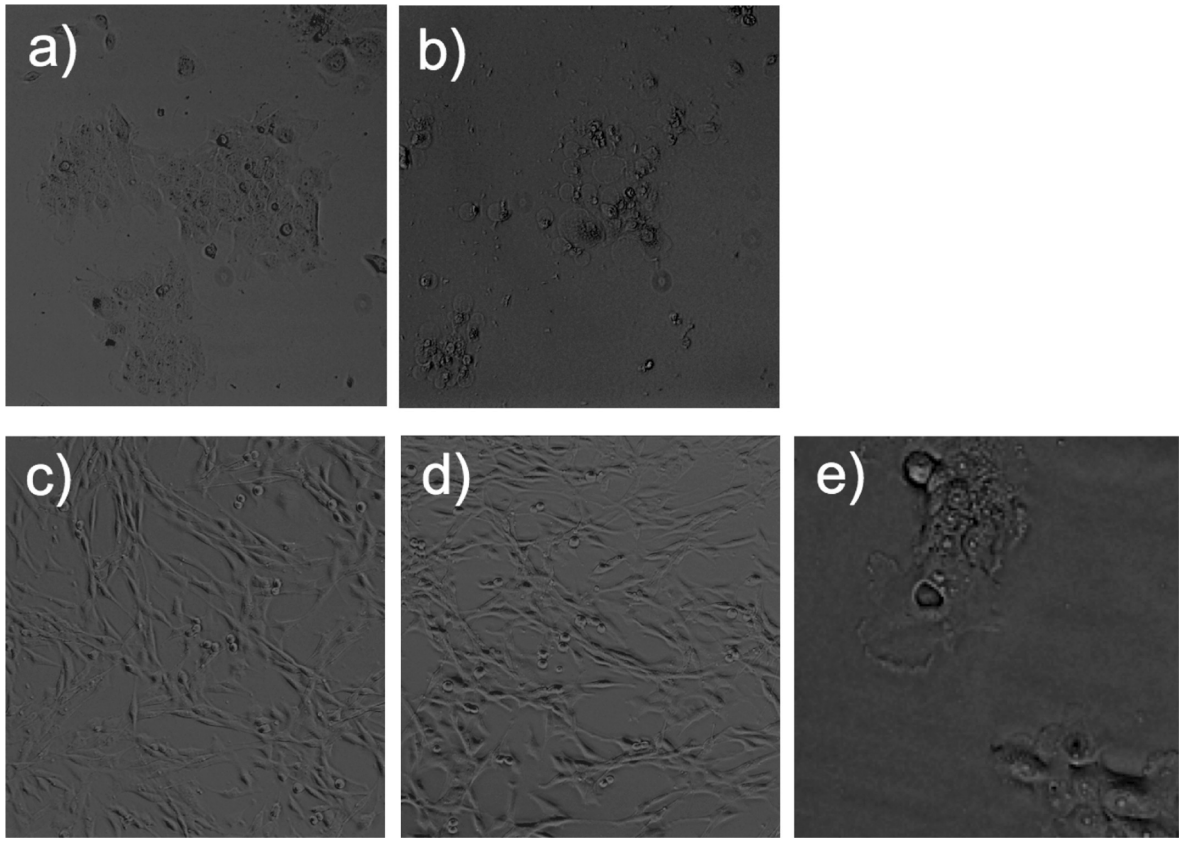

Figure 5. Cell viability by treatment with **1ii** and **1** (10 μM) at 37 °C for 6 h (PH-detection). (a) Control A431 cells. (b) Treatment of A431 with **1ii**. (c) Control C6 glioma cells. (d) Treatment of C6 cells with **1ii**. (e) Treatment of A431 cells with **1**. PH: phase-contrast image.

discussion). Phosphorylation of EGF, Gab1, Shc, and IRS-1 are recognized by the Garb2-SH2 domain,[22−24] whereas phosphorylated CAS and CBL interact with the CrkL-SH2 domain.[77−79] Only the anti-Shc antibody was detected using the biotin-probe at the band position 65 kDa, which was the same band observed during reverse staining (Figure 4B); although we tried the blotting experiments in Figure 4B with only two concentrations, the Shc band intensity was apparently and reproducibly enhanced when the concentration of the biotin sample was increased. Thus, phosphorylated Shc was suggested to be one of the candidates for selective interaction with the clicked product **1ii**.

In further proving the interaction with p-Shc in the A431 cells, the homogenized A431 cells in Figure 3 were treated with the antibodies, and the antibody complexes were then fished out by proteinA-agarose (Supplementary Figure S6). Direct detection of the fluorescence on agarose/antibodies showed much higher intensity for the α-Shc antibody than those of α-actin and α-IgG antibodies used for the controls, thus proving the preferential interaction of **1ii** with Shc in the cells.

We were delighted to find that the clicked peptide **1ii** induced selective cytotoxicity to the A431 cancer cells in the *in vitro* experiments. Incubation with 10 μM peptide **1ii** led to cell death within 6 h (Figure 5a,b). Cytotoxic effects of **1ii** on A431 cells were also evaluated by the microtiter plate assay (MTT assay)[80,81] of dose−response behavior with the colorimetric readout (Supplementary Figure S7). In clear contrast, no relevant changes in appearance were observed in the EGFR-independent tumor cell line, the C6 glioma cells,[82] even though the peptide **1ii** was internalized into the cells (Figure 5c,d, Supplementary Figure S5). The simpler peptide **1**, which was a precursor for the click reaction (after cleavage from the resin), did not cause cell death in the A431 cell culture (Figure 5e). The clicked product **1ii** therefore appeared to selectively bind and interrupt the target phosphorylated proteins of the SH2 domain in the EGFR-mediated signaling pathway,[22−24] *e.g.*, *p*-Shc. This clicked product, therefore, introduced selective cytotoxicity into the A431 cancer cells.

It should be noted that the clicked peptide **1ii** also exhibited A431-selective inhibition of tumor growth in the preliminary animal experiments[83] (Figure 6, Methods). The peptide **1ii** was intravenously administrated to the A431-implanted BALB/c nude mice over 7 days, maintaining a peptide blood concentration of 100 μM (a factor of 10 higher concentration than the cell-based experiments described in Figure 5). Peptide **1ii** selectively inhibited the tumor growth of A431-implanted mice, whereas toxic effects of **1ii** were not observed; there was not significant change in the time course of the animal weight (Supplementary Figure S10). Furthermore, no inflammatory responses could be observed during the *in vivo* experiments, on the basis of the organ histological data on liver, kidney, and spleen (Supplementary Figure S11). Although tumor growth was inhibited by 73 vol %, a comparison with the control experiments, in which saline was administered (Figure 6a), showed that the weights of other normal organs, such as the brain, heart, lung, liver, spleen, and kidney, remained unchanged (Figure 6b). Furthermore, peptide **1ii** did not affect the tumor growth in the C6 cell-implanted mice (Figure 6c,d). Thus, the clicked peptide's selectivity, gained by the template-assisted protocol, worked well in an *in vivo* study.

In conclusion, we have developed a template-assisted approach to developing artificial receptors that can selectively

dx.doi.org/10.1021/cb2003175 | *ACS Chem. Biol.* 2012, 7, 637−645

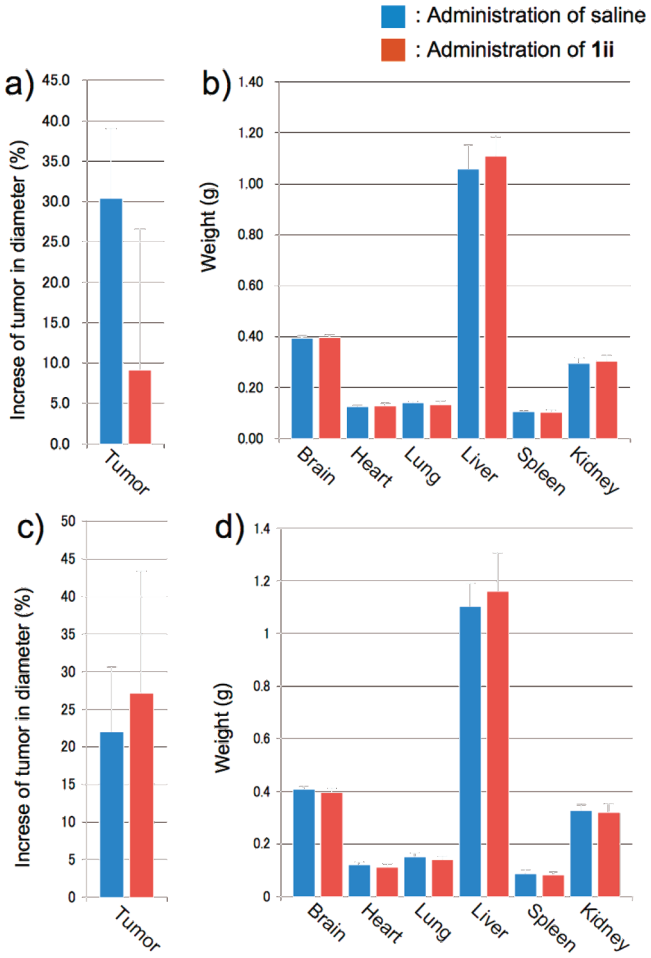

Figure 6. Anticancer activity of **1ii** in A431- and C6 glioma-implanted BALB/c mice (N = 4). The diameter of the tumor and weight of the other organs were measured after dissection. Red bar: administration of **1ii**. Blue bar: administration of saline instead of **1ii**. t test with the significance level at $p < 0.05$ was set to assess the statistical significance. For **1ii** administration in A431-implanted mice, a significant decrease was not found, but a trend of decrease was observed (p = 0.07). For **1ii** administration in C6 glioma-implanted mice, on the other hand, no significant difference was found (p = 0.56). (a) Increase in the tumor diameter (%) before and after 7-day administration to A431-implanted mice. (b) Comparison of organ weight after the 7-day administration to A431-implanted mice. (c) Increase in tumor diameter (%) before and after administration in C6 glioma-implanted mice. (d) Comparison of organ weight after administration to C6 glioma-implanted mice.

interrupt phosphorylation-mediated protein/protein interactions. As a model case, the peptidyl mimic of the Grb2-SH2 domain was found to be internalized into A431 cancer cells, where it selectively bound to the Grb2-SH2 interacting signaling proteins, induced A431-selective cytotoxicity, and exhibited tumor growth inhibition *in vivo*. The present strategy must be improved to increase the binding affinity of **1ii** to the template peptide **3a**, thereby enhancing the *in vitro* and *in vivo* bioactivity. However, the results described here demonstrate the tailor-made synthesis of artificial receptors using a method that is clearly distinct from previous methods. This approach may efficiently and rapidly provide small-molecular regulators that selectively control a specific cell signaling pathway or protein/protein interactions. Further chemical-biology-directed research based on the presented method is currently underway in our laboratory.

METHODS

Synthesis of Peptides and Their Labeled Derivatives. Detailed synthetic procedures and characterizations are described in the Supporting Information.

General Procedure for the Template-Assisted and Self-Activating Click Reaction. To the suspension of bis-lysine **1** immobilized on the Wang resin (2.0 mg, 1.0 μmol) in dry THF (720 μL) were added the cyclic peptide **3a** (700 μg, 1.0 μmol) in MeCN (50 μL) and H_2O (50 μL) at RT. After the mixture was shaken for 1 h, a suspension of TFA salts of H-Leu-Lys-Phe-Pra-OH **2e** (1.0 mg, 2.0 μmol), H-Ser-His-Asn-Pra-OH **2i** (1.0 mg, 2.0 μmol), H-Asn-Lys-Phe-Pra-OH **2j** (1.0 mg, 2.0 μmol), and CuI (1.0 mg, 6.0 μmol) in DMF (80 μL) was added at RT. After the resulting mixture was shaken at RT for 5 d, the resin was washed with DMF (1.5 mL, 2.0 min, 5 times), H_2O (1.5 mL, 2.0 min, 3 times), DOTA in H_2O (2.0 mg in 1.5 mL, 5.0 μmol, 1 h), H_2O (1.5 mL, 2.0 min, 5 times), DMF (1.5 mL, 2.0 min, 3 times), CH_2Cl_2 (1.5 mL, 2.0 min, 3 times), and finally with diethyl ether (1.5 mL, 2.0 min, 3 times). The resin was dried *in vacuo* for 3 h, and then it was treated with 2.0 mL TFA/TES/H_2O (31:1:1). After the mixture was shaken at RT for 30 min, the resulting solution was filtered, the filtrate was concentrated *in vacuo*, lyophilized from MeCN/H_2O, and analyzed by HPLC (column: Nacalai tesque $5C_{18}$-AR300, 4.6 mm × 250 mm; MeCN in H_2O (50−100% gradient over 60 min) and ESI- and MALDI-MS. Data for **1ii**: $[\alpha]^{23}_D$ +1.6° (c 0.5, MeOH); IR (neat, cm^{-1}) 3050 (br), 1674, 1542, 1203, 1135; ^1H NMR (D_2O) δ 8.59 (d, J = 5.7 Hz, 2H), 8.46 (s, 2H), 7.67 (s, 2H), 7.30 (brs, 4H), 7.19 (brs, 5H), 7.14 (s, 2H), 5.20 (s, 4H), 4.54 (m, 2H), 4.50−4.44 (m, 2H), 4.20 (m, 2H), 4.13 (m, 2H), 3.99 (m, 2H), 3.87 (t, J = 6.4 Hz, 1H), 3.81 (m, 2H), 3.71 (m, 1H), 3.61 (m, 2H), 3.12 (m, 2H), 3.01 (m, 5H), 2.83 (m, 4H), 2.59 (dd, J = 14.0, 4.9 Hz, 2H), 2.51 (dd, J = 14.0, 9.0 Hz, 2H), 1.76−1.69 (m, 6H), 1.57−1.48 (m, 8H), 1.36−1.29 (m, 3H), 1.19 (m, 3H); ^{13}C NMR (D_2O; compound **1ii** exists as the amide rotamers (see a copy of the spectrum in Supplementary Figure S1)) δ 176.4, 174.6, 174.5, 174.4, 173.5, 173.4, 172.4, 172.2, 172.1, 172.1, 171.5, 171.2, 171.0, 170.4, 168.4, 168.4, 163.9, 163.6, 163.4, 163.1, 143.5, 135.2, 135.2, 134.4, 134.2, 129.9, 129.8, 129.8, 128.9, 128.9, 128.7, 125.0, 120.9, 120.4, 118.1, 117.9, 115.8, 113.5, 60.7, 55.0, 54.0, 53.6, 53.3, 53.2, 51.0, 50.1, 42.9, 42.5, 39.7, 39.6, 37.0, 36.9, 31.0, 30.8, 28.4, 27.3, 27.0, 26.9, 26.7, 26.3, 22.9, 21.8; HRESI-MS m/z calcd for $C_{94}H_{138}N_{36}O_{24}$ $(M + 2H)^{2+}$ 1077.5336, found1077.5242.

Interaction between Clicked Peptides and Phosphopeptide 3b; Procedure of Dissociation Constants (K_d). To a 1.45×10^{-4} M solution (100 μL, H_2O) of the peptide **1ii** or **1jj** was added the fluorescence peptide **3b** at a concentration ranging from 1.39×10^{-6} M to 8.90×10^{-4} M (100 μL, H_2O) at RT, and the mixture was shaken for 24 h at RT. Change in the coumarin fluorescence intensity at 552 nm was plotted against the concentrations of **3b** (see Supplementary Figure S4), and the standard curve was obtained. K_d was then calculated on the basis of the Scatchard plots; titration was performed three times for each peptide **1ii** and **1jj**, and the K_d value was averaged.

Preparation of 431 Cell Lysate. Cells were pelleted and resuspended in ice-cold lysis buffer (1% Triton X-100/50 mM β-glycerophosphate/1.5 mM EGTA/0.5 mM EDTA/5% glycerol/25 mM Tris HCl, pH 7.4) in the presence of protease inhibitors cocktail (Complete; Roche, Diagnostic, Germany), and the resulting lysates were cleared by centrifugation. The protein concentrations were measured based on the BCA methods and stored at −80 °C before use.

Identification of 1ii-Interacting Protein from A431 Lysates. Detailed procedures for avidin bead extraction of **1ii**-interacting proteins, SDS-PAGE, reverse staining, Western blotting, and antibody-detection are described in the Supporting Information.

Animal Experiments for Tumor Growth Inhibition. The human epidermoid carcinoma cell line A431 (RCB0202) was provided by the RIKEN BRC through the National Bio-Resource Project of the

dx.doi.org/10.1021/cb2003175 | ACS Chem. Biol. 2012, 7, 637−645

MEXT, Japan. The cells were cultured at 37 °C under a 5% CO_2 atmosphere in Dulbecco's Modified Eagle's Medium (DMEM) supplemented with 10% fetal bovine serum, 100 U/mL penicillin, and 100 μg/mL streptomycin. Cells were regularly certified as free of Mycoplasma contamination.

Athymic Female BALB/c nude mice (8 weeks old, weighing 18−20 g) were obtained from Japan SLC, Inc. (Shizuoka, Japan) and provided with water and normal chow. Animals were housed in an air-conditioned room at 21−26 °C with 45−55% moisture and a 12h dark/light cycle. The A431 tumor cells (5.0×10^6 cells/0.1 mL) were implanted subcutaneously in the right dorsal region of the mice. When tumors reached a size of 40−50 mm^3 (width^2 × length/2), the mice were randomly separated into two groups (n = 6 each) to receive clicked peptide **1ii** (dissolved in 0.9% saline) at the dose of 22 mg/kg/day. In contrast, negative controls received saline, respectively, all administered intravenously for 7 days. Tumor size was measured every day. On day 8, mice were sacrificed by cervical dislocation and their organs (brain, heart, lung, kidneys, spleens, and livers), and tumors were dissected out and weighed. All animal studies were conducted in accordance with the Guidelines of the RIKEN for animal research and the protocol approved by the study review committee of this institute.

■ ASSOCIATED CONTENT

Supporting Information

This material is available free of charge *via* the Internet at http://pubs.acs.org.

■ AUTHOR INFORMATION

Corresponding Author

*E-mail: ktzenori@chem.sci.osaka-u.ac.jp, koichi@chem.sci.osaka-u.ac.jp.

Notes

The authors declare no competing financial interest.

■ ACKNOWLEDGMENTS

This work was supported in part by Grants-in-Aid for Scientific Research No. 19681024 and 19651095 from the Japan Society for the Promotion of Science, Collaborative Development of Innovative Seeds from the Japan Science and Technology Agency (JST), New Energy and Industrial Technology Development Organization (NEDO, project ID: 07A01014a), Research Grants from the Yamada Science Foundation and Japan Peptide Science Foundation as well as the Molecular Imaging Research Program, Grants-in-Aid for Scientific Research from the Ministry of Education, Culture, Sports, Science and Technology (MEXT) of Japan.

■ REFERENCES

(1) Peczuh, M. W., and Hamilton, A. D. (2000) Peptide and protein recognition by designed molecules. *Chem. Rev. 100*, 2479−2493.

(2) Fazal, M. A., Roy, B. C., Sun, S., Mallik, S., and Rodgers, K. R. (2001) Surface recognition of a protein using designed transition metal complexes. *J. Am. Chem. Soc. 123*, 6283−6290.

(3) Gradl, S. N., Felix, J. P., Isacoff, E. Y., Garcia, M. L., and Trauner, D. (2003) Protein surface recognition by rational design: Nanomolar ligands for potassium channels. *J. Am. Chem. Soc. 125*, 12668−12669.

(4) Jain, R., Ernst, J. T., Kutzki, O., Park, Y. S., and Hamilton, A. D. (2004) Protein recognition using synthetic surface-targeted agents. *Mol. Divers. 8*, 89−100.

(5) Yin, H., and Hamilton, A. D. (2005) Strategies for targeting protein−protein interactions with synthetic agents. *Angew. Chem., Int. Ed. 44*, 4130−4163.

(6) Fletcher, S., and Hamilton, A. D. (2005) Protein surface recognition and proteomimetics: mimics of protein surface structure and function. *Curr. Opin. Chem. Biol. 9*, 632−638.

(7) Fletcher, S., and Hamilton, A. D. (2006) Targeting protein−protein interactions by rational design: mimicry of protein surfaces. *J. R. Soc. Interface 3*, 215−233.

(8) Ojida, A., Inoue, M., Mito-oka, Y., Tsutsumi, H., Sada, K., and Hamachi, I. (2006) Effective disruption of phosphoprotein−protein surface interaction using Zn(II) dipicolylamine-based artificial receptors via two-point Interaction. *J. Am. Chem. Soc. 128*, 2052−2058.

(9) Davis, J. M., Tsou, L. K., and Hamilton, A. D. (2007) Synthetic non-peptide mimetics of α-helices. *Chem. Soc. Rev. 36*, 326−334.

(10) Yin, H., Hamilton, A. D. (2007) Protein secondary structure mimetics as modulators of protein-protein and protein-ligand interactions. In *Chemical Biology: From Small Molecules to Systems Biology and Drug Design* (Schreiber, S. L., Kapoor, T. M., and Wess, G., Ed.), 1st ed., Vol. *1*, pp 250−269, Wiley-VCH, Weinheim.

(11) Saraogi, I., and Hamilton, A. D. (2008) α-Helix mimetics as inhibitors of protein−protein interactions. *Biochem. Soc. Trans. 36*, 1414−1417.

(12) Haydar, S. N., Yun, H. S., Roland, G. W., and Hirst, W. D. (2009) Small-molecule protein−protein interaction inhibitors as therapeutic agents for neurodegenerative diseases: Recent progress and future directions. *Annu. Rep. Med. Chem. 44*, 51−69.

(13) Bovens, S., and Ottmann, C. (2009) Modulation of protein−protein interactions by small molecules. *Chem. Biol.*, 105−119.

(14) Wilson, A. J. (2009) Inhibition of protein−protein interactions using designed molecules. *Chem. Soc. Rev. 38*, 3289−3300.

(15) Whitty, A. (2009) Small Molecule Inhibitors of Protein-Protein Interactions: Challenges and Prospects, In *Gene Family Targeted Molecular Design* (Lackey, K. E., Ed.), 1st ed., pp 199−233, Wiley-Interscience, Hoboken.

(16) Berg, T. (2009) Protein−Protein Interaction: Modulation with Small Molucules. In *Wiley Encyclopedia of Chemical Biology* (Begley, T. P., Ed.), 1st ed., Vol. *4*, pp 121−143, Wiley-Interscience, Hoboken.

(17) Guessous, F., Zhang, Y., diPierro, C., Marcinkiewicz, L., Sarkaria, J., Schiff, D., Buchanan, S., and Abounader, R. (2010) An orally bioavailable c-Met kinase inhibitor potently inhibits brain tumor malignancy and growth. *Anticancer Agents Med. Chem. 10*, 28−35.

(18) Lok, W., Klein, R. Q., and Saif, M. W. (2010) Aurora kinase inhibitors as anti-cancer therap. *Anticancer Drugs 21*, 339−350.

(19) Krishnamurty, R., and Maly, D. J. (2010) Biochemical mechanisms of resistance to small-molecule protein kinase inhibitors. *ACS Chem. Biol. 5*, 121−138.

(20) Galons, H., Oumata, N., and Meijer, L. (2010) Cyclin-dependent kinase inhibitors: a survey of recent patent literature. *Expert Opin. Ther. Pat. 20*, 377−404.

(21) Ghayad, S. E., and Cohen, P. A. (2010) Inhibitors of the PI3K/Akt/mTOR pathway: New hope for breast cancer patients. *Recent Pat. Anticancer Drug Discov. 5*, 29−57.

(22) Lowenstein, E. J., Daly, R. J., Batzer, W. L., Margolis, B., Lammers, R., Ullrich, A., Skolnik, E. Y., Bar-Sagi, D., and Schlessinger, J. (1992) A novel transforming protein (SHC) with an SH2 domain is implicated in mitogenic signal transduction. *Cell 70*, 431−442.

(23) Downward, J. (1994) The GRB2/Sem-5 adaptor protein. *FEBS Lett. 338*, 113−117.

(24) Chardin, P., Cussac, D., Maigan, S., and Ducruix, A. (1995) The Grb2 adaptor. *FEBS Lett. 369*, 47−51.

(25) Gishizky, M. L. (1995) Chapter 26. Tyrosine Kinase Induced Mitogenesis Breaking the Link With Cancer. In *Annual Reports in Medicinal Chemistry* (Bristol, J. A., Ed.), Vol. *30*, pp 247−253, Academic Press, San Diego.

(26) Smithgall, T. E. (1995) SH2 and SH3 domains: Potential targets for anti-cancer drug design. *J. Pharmacol. Toxicol. Methods 34*, 125−132.

(27) Beattie, J. (1996) SH2 domain protein interaction and possibilities for pharmacological intervention. *Cell Signal. 8*, 75−86.

(28) Mandal, P. K., Gao, F., Lu, Z., Ren, Z., Ramesh, R., Birtwistle, J. S., Kaluarachchi, K. K., Chen, X., Bast, R. C. Jr., Liao, W. S., and McMurray, J. S. (2011) Potent and selective phosphopeptide mimetic prodrugs targeted to the Src Homology 2 (SH2) domain of signal

transducer and activator of transcription 3. *J. Med. Chem. 54*, 3549−3563.
(29) Hart, C. P., Martin, J. E., Reed, M. A., Keval, A. A., Pustelnik, M. J., Northrop, J. P., Patel, D. V., and Grove, J. R. (1999) Potent inhibitory ligands of the GRB2 SH2 domain from recombinant peptide libraries. *Cell. Signal. 11*, 453−464.
(30) Ettmayer, P., France, D., Gounarides, J., Jarosinski, M., Martin, M.-S., Rondeau, J.-M., Sabio, M., Topiol, S., Weidmann, B., Zurini, M., and Bair, K. W. (1999) Structural and conformational requirements for high-affinity binding to the SH2 domain of Grb2. *J. Med. Chem. 42*, 971−980.
(31) Long, Y.-Q., Lung, F.-D. T., and Roller, P. P. (2003) Global optimization of conformational constraint on non-phosphorylated cyclic peptide antagonists of the Grb2-SH2 domain. *Bioorg. Med. Chem. 11*, 3929−3936.
(32) Li, P., Peach, M. L., Zhang, M., Liu, H., Yang, D., Nicklaus, M., and Roller, P. P. (2003) Structure-based design of thioether-bridged cyclic phosphopeptides binding to Grb2-SH2 domain. *Bioorg. Med. Chem. Lett. 13*, 895−899.
(33) Shi, Y.-h., Song, Y.-L., Lin, D.-h., Tan, J., Roller, P. P., Li, Q., Long, Y.-Q., and Song, G.-Q. (2005) Binding affinity difference induced by the stereochemistry of the sulfoxide bridge of the cyclic peptide inhibitors of Grb2-SH2 domain: NMR studies for the structural origin. *Biochem. Biophys. Res. Commun. 330*, 1254−1261.
(34) Vidal, M., Gigoux, V., and Garbay, C. (2001) SH2 and SH3 domains as targets for anti-proliferative agents. *Crit. Rev. Oncol. Hematol. 40*, 175−186.
(35) Song, Y.-L., Peach, M. L., Roller, P. P., Qiu, S., Wang, S., and Long, Y.-Q. (2006) Discovery of a novel nonphosphorylated pentapeptide motif displaying high affinity for Grb2-SH2 domain by the utilization of 3′-substituted tyrosine derivatives. *J. Med. Chem. 49*, 1585−1596.
(36) Rahuel, J., Gay, B., Erdmann, D., Strauss, A., Garcia-Echeverria, C., Furet, P., Caravatti, G., Fretz, H., Schoepfer, J., and Grutter, M. G. (1996) Structural basis for specificity of GRB2-SH2 revealed by a novel ligand binding mode. *Nat. Struct. Biol. 3*, 586−589.
(37) Rahuel., J., Garcia-Echeverria, C., Furet, P., Strauss, A., Caravatti, G., Fretz, H., Schoepfer, J., and Gay, B. (1998) Structural basis for the high affinity of amino-aromatic SH2 phosphopeptide ligands. *J. Mol. Biol. 279*, 1013−1022.
(38) Furet, P., Garcia-Echeverria, C., Gay, B., Schoepfer, J., Zeller, J., and Rahuel, J. (1999) Structure-based design, synthesis, and X-ray crystallography of a high-affinity antagonist of the Grb2-SH2 domain containing an asparagine mimetic. *J. Med. Chem. 42*, 2358−2363.
(39) Schiering, N., Casale, E., Caccia, P., Giordano, P., and Battistini, C. (2000) Dimer formation through domain swapping in the crystal structure of the Grb2-SH2−Ac-pYVNV Complex. *Biochem. 39*, 13376−13382.
(40) Fukase, K., Wakao, M., Izumi, M., Ueno, A., Oikawa, M., Suda, Y., Kusumoto, S., Nestler, H. P., Sherlock, R., and Liu, R. (2001) Identification of branched peptidic structures that recognize immunostimulating glycoconjugate lipid A from encoded combinatorial libraries. *Peptide Sci. 2000*, 365−368.
(41) Huc, I., and Lehn, J.-M. (1997) Virtual combinatorial libraries: Dynamic generation of molecular and supramolecular diversity by self-assembly. *Proc. Natl. Acad. Sci. U.S.A. 94*, 2106.
(42) Kolb, H. C., Finn, M. G., and Sharpless, K. B. (2001) Click chemistry: Diverse chemical function from a few good reactions. *Angew. Chem., Int. Ed. 40*, 2004−2021.
(43) Kolb, H. C., and Sharpless, K. B. (2003) The growing impact of click chemistry on drug discovery. *Drug Discovery Today 8*, 1128−1137.
(44) Tornoe, C. W., Christensen, C., and Meldal, M. (2002) Peptidotriazoles on solid phase: [1,2,3]-Triazoles by regiospecific copper(I)-catalyzed 1,3-dipolar cycloadditions of terminal alkynes to azides. *J. Org. Chem. 67*, 3057−3064.
(45) Rostovtsev, V. V., Green, L. G., Fokin, V. V., and Sharpless, K. B. (2002) A stepwise Huisgen cycloaddition process: Copper(I)-catalyzed regioselective "ligation" of azides and terminal alkynes. *Angew. Chem., Int. Ed. 41*, 2596−2599.
(46) Bock, V. D., Hiemstra, H., and van Maarseveen, J. H. (2006) Cu^{I}-catalyzed alkyne−azide "click" cycloadditions from a mechanistic and synthetic perspective. *Eur. J. Org. Chem. 6*, 51−68.
(47) Rodionov, V. O., Presolski, S. I., Gardinier, S., Lim, Y.-H., and Finn, M. G. (2007) Benzimidazole and related ligands for Cu-catalyzed azide-alkyne cycloaddition. *J. Am. Chem. Soc. 129*, 12696−12704.
(48) Hong, V., Presolski, S. I., Ma, C., and Finn, M. G. (2009) Analysis and optimization of copper-catalyzed azide-alkyne cycloaddition for bioconjugation. *Angew. Chem., Int. Ed. 48*, 9879−9883.
(49) Presolski, S. I., Hong, V., Cho, S.-H., and Finn, M. G. (2010) Tailored ligand acceleration of the Cu-catalyzed azide−alkyne cycloaddition reaction: Practical and mechanistic implications. *J. Am. Chem. Soc. 132*, 14570−14576.
(50) Manetsch, R., Krasinski, A., Radic, Z., Raushel, J., Taylor, P., Sharpless, K. B., and Kolb, H. C. (2004) In situ click chemistry: Enzyme inhibitors made to their own specifications. *J. Am. Chem. Soc. 126*, 12809−12818.
(51) Mocharla, V. P., Colasson, B., Lee, L. V., Roeper, S., Sharpless, K. B., Wong, C.-H., and Kolb, H. C. (2005) In situ click chemistry: Enzyme-generated inhibitors of carbonic anhydrase II. *Angew. Chem., Int. Ed. 44*, 116−120.
(52) Krasinski, A., Radic, Z., Manetsch, R., Raushel, J., Taylor, P., Sharpless, K. B., and Kolb, H. C. (2005) In situ selection of lead compounds by click chemistry: Target-guided optimization of acetylcholinesterase inhibitors. *J. Am. Chem. Soc. 127*, 6686−6692.
(53) Whiting, M., Muldoon, J., Lin, Y.-C., Silverman, S. M., Lindstrom, W., Olson, A. J., Kolb, H. C., Finn, M. G., Sharpless, K. B., Elder, J. H., and Fokin, V. V. (2006) Inhibitors of HIV-1 protease by using in situ click chemistry. *Angew. Chem., Int. Ed. 45*, 1435−1439.
(54) Wang, J., Sui, G., Mocharla, V. P., Lin, R. J., Phelps, M. E., Kolb, H. C., and Tseng, H.-R. (2006) Integrated microfluidics for parallel screening of an in situ click chemistry library. *Angew. Chem., Int. Ed. 45*, 5276−5281.
(55) Sharpless, K. B., and Manetsch, R. (2006) *In situ* click chemistry: A powerful means for lead discovery. *Expert Opin. Drug Discovery*, 525−538.
(56) Hirose, T., Sunazuka, T., Sugawara, A., Endo, A., Iguchi, K., Yamamoto, T., Ui, H., Shiomi, K., Watanabe, T., Sharpless, K. B., and Omura, S. (2009) Chitinase inhibitors: Extraction of the active framework from natural argifin and use of *in situ* click chemistry. *J. Antibiot. 62*, 277−282.
(57) Agnew, H. D., Rohde, R. D., Millward, S. W., Nag, A., Yeo, W.-S., Hein, J. E., Pitram, S. M., Tariq, A. A., Burns, V. M., Krom, R. J., Fokin, V. V., Sharpless, K. B., and Heath, J. R. (2009) Iterative in situ click chemistry creates antibody-like protein-capture agents. *Angew. Chem., Int. Ed. 48*, 4944−4948.
(58) Mamidyala, S. K., and Finn, M. G. (2010) *In situ* click chemistry: probing the binding landscapes of biological molecules. *Chem. Soc. Rev. 39*, 1252−1261.
(59) Hu, X., and Manetsch, R. (2010) Kinetic target-guided synthesis. *Chem. Soc. Rev. 39*, 1316−24.
(60) Tanaka, K., Kageyama, C., and Fukase, K. (2007) Acceleration of Cu(I)-mediated Huisgen 1,3-dipolar cycloaddition by histidine derivatives. *Tetrahedron Lett. 48*, 6475−6479.
(61) Tanaka, K., Siwu, E. R. O., Minami, K., Hasegawa, K., Nozaki, S., Kanayama, Y., Koyama, K., Chen, W., Paulson, J. C., Watanabe, Y., and Fukase, K. (2010) Non-invasive imaging of dendrimer-type *N*-glycan clusters: remarkable in vivo dynamics dependence on oligosaccharide structure. *Angew. Chem., Int. Ed. 49*, 8195−8200.
(62) Tanaka, K., and Fukase, K. (2008) PET (positron emission tomography) imaging of biomolecules using metal−DOTA complexes: a new collaborative challenge by chemists, biologists, and physicians for future diagnostics and exploration of *in vivo* dynamics. *Org. Biomol. Chem. 6*, 815−828.
(63) Tanaka, K., and Fukase, K. (2008) Recent advances in positron emission tomography (PET) imaging of biomolecules: From chemical labeling to cancer diagnostics. *Mini-Rev. Org. Chem. 5*, 153−162.

(64) Shobini, J., Mishra, A. K., Sandhya, K., and Chandra, N. (2001) Interaction of coumarin derivatives with human serum albumin: investigation by fluorescence spectroscopic technique and modeling studies. *Spectrochim. Acta Part A 57*, 1133−1147.
(65) Tian, J., Liu, J., Hu, Z., and Chen, X. (2005) Interaction of wogonin with bovine serum albumin. *Bioorg. Med. Chem. 13*, 4124−4129.
(66) Guo, L., Qiu, B., and Chen, G. (2007) Synthesis and investigation on the interaction with calf thymus deoxyribonucleic acid of a novel fluorescent probe 7-oxobenzo[*b*][1,10]phenanthroline-12(7H)-sulfonic acid. *Anal. Chim. Acta 588*, 123−130.
(67) Bharathi., and Rao, K. S. J. (2008) Molecular understanding of copper and iron interaction with α-synuclein by fluorescence Analysis. *J. Mol. Neurosci. 35*, 273−281.
(68) Carpenter, G., King, L. Jr., and Cohen, S. (1978) Epidermal growth factor stimulates phosphorylation in membrane preparations in vitro. *Nature 276*, 409−410.
(69) Futaki, S. (2006) Oligoarginine vectors for intracellular delivery: Design and cellular-uptake mechanisms. *Biopolymers 84*, 241−249.
(70) Futaki, S., Nakase, I., Tadokoro, A., Takeuchi, T., and Jones, A. T. (2007) Arginine-rich peptides and their internalization mechanisms. *Biochem. Soc. Trans. 35*, 784−787.
(71) El-Sayed, A., Futaki, S., and Harashima, H. (2009) Delivery of macromolecules using arginine-rich cell-penetrating peptides: Ways to overcome endosomal entrapment. *AAPS J. 11*, 13−22.
(72) Matsui, N. M., Smith-Beckerman, D. M., Epstein, L. B. (1999) Staining of Preparative 2-D Gels. In *2-D Proteome Analysis Protocols (Methods in Molecular Biology* (Link, A. J., Ed.), 1st ed., pp 307−311, Humana Press, New York.
(73) Cohen, S. L., and Chait, B. T. (1997) Mass spectrometry of whole proteins eluted from sodium dodecyl sulfate−polyacrylamide gel electrophoresis gels. *Anal. Biochem. 247*, 257−267.
(74) Qi, Y., and Katagiri, F. (2009) Purification of low-abundance Arabidopsis plasma-membrane protein complexes and identification of candidate components. *The Plant Journal 57*, 932−944.
(75) Gureel, C., Vercoutter-Edouart, A.-S., Fonbonne, C., Mortuaire, M., Salvador, A., Michalski, H.-C., and Lemoine, J. (2008) Identification of new *O* -GlcNAc modified proteins using a click-chemistry-based tagging. *Anal. Bioanal. Chem. 390*, 2089−2097.
(76) Tamura, S., Shiomi, A., Kaneko, M., Ye, Y., Yoshida, M., Yoshikawa, M., Kimura, T., Kobayashi, M., and Murakami, N. (2009) New Rev-export inhibitor from *Alpinia galanga* and structure−activity relationship. *Bioorg. Med. Chem. Lett. 19*, 2555−2557.
(77) Sattler, M., and Salgia, R. (1998) Role of the adapter protein CRKL in signal transduction of normal hematopoietic and BCR/ABL-transformed cells. *Leukemia 12*, 637−644.
(78) Seo, J.-H., Suenaga, A., Hatakeyama, M., Taiji, M., and Imamoto, A. (2009) Structural and functional basis of a role for CRKL in a fibroblast growth factor 8-induced feed-forward loop. *Mol. Cell. Biol. 29*, 3076−3087.
(79) Mintz, P. J., Cardó-Vila, M., Ozawa, M. G., Hajitou, A., Rangel, R., Guzman-Rojas, L., Christianson, D. R., Arap, M. A., Giordano, R. J., Souza, G. R., Easley, J., Salameh, A., Oliviero, S., Brentani, R. R., Koivunen, E., Arap, W., and Pasqualini, R. (2009) An unrecognized extracellular function for an intracellular adapter protein released from the cytoplasm into the tumor microenvironment. *Proc. Natl. Acad. Sci. U.S.A. 106*, 2182−2187.
(80) Ishiyama, M., Miyazono, Y., Sasamoto, K., Ohkura, Y., and Ueno, K. (1997) A highly water-soluble disulfonated tetrazolium salt as a chromogenic indicator for NADH as well as cell viability. *Talanta 44*, 1299.
(81) Tominaga, H., Ishiyama, M., Ohseto, F., Sasamoto, K., Hamamoto, T., Suzuki, K., and Watanabe, M. (1999) A water-soluble tetrazoliumsalt useful for colorimetric cell viability assay. *Anal. Commun. 36*, 47−50.
(82) Grobben, B., De Deyn, P. P., and Slegers, H. (2002) Rat C6 glioma as experimental model system for the study of glioblastoma growth and invasion. *Cell Tissue Res. 310*, 257−270.
(83) LaMontagne, K. R., Butler, J., Borowski, V. B., Fuentes-Pesquera, A. R., Blevitt, J. M., Huang, S., Li, R., Connolly, P. J., and Greenberger, L. M. (2009) A highly selective, orally bioavailable, vascular endothelial growth factor receptor-2 tyrosine kinase inhibitor has potent activity in vitro and in vivo. *Angiogenesis 12*, 287−296.